

18.2 A Single-Chip Dual-Band 22-to-29GHz/77-to-81GHz BiCMOS Transceiver for Automotive Radars

Vipul Jain, Fred Tzeng, Lei Zhou, Payam Heydari

University of California, Irvine, CA

In the last few years, silicon-based 24GHz short-range automotive radars have been investigated both by industry and academia [1,2]. Intensive research/development is also underway for developing 77GHz long-range [3] and 77-to-81GHz short-range radars [4] in silicon technologies. While ETSI will discontinue the use of the 24GHz allocation for automotive short-range sensors in mid-2013 [5], thereafter mandating a shift to 79GHz, mature 24GHz technology will continue to dominate non-European markets. Therefore, next-generation radar sensors may well be required to support both frequency bands, for compatibility and lower overall cost. This paper presents a dual-band millimeter-wave (mmWave) transceiver (TRX) in a 0.18 μ m BiCMOS technology ($f_T/f_{max}=200/180$ GHz). The dual-band TRX operates in the 22-to-29GHz and 77-to-81GHz short-range automotive radar bands.

The dual-band TRX is based on the direct-conversion pulsed-radar architecture shown in Fig. 18.2.1. Circuits in the frequency synthesizer, pulse generator and downconversion chain are shared between the two bands, resulting in a lower overall chip area. The radar transmits RF pulses at a rate determined by the pulse repetition frequency (*prf*). The presence of an object is detected in the RX by correlating the reflected pulse with a delayed version of the transmitted pulse. To detect targets over a wide range of 0.15 to 40m, it is necessary to have a widely-tunable delay between pulse transmission and receiver correlation. Moreover, to achieve longer range and higher range resolution, it is necessary to incorporate variable *prf* and pulse width. To meet these requirements, the CMOS base-band pulse generator in Fig. 18.2.1 can generate pulses with widths ranging from 200ps to 2ns ($pw[5:0]$), with a variable *prf* of 1MHz to 1.5GHz ($prf[12:0]$). The delay between TX and RX triggers can be tuned from 1ns to 0.3 μ s ($delay[12:0]$), corresponding to the 0.15-to-40m radar range. The *prf* generation circuitry is clocked by the 100MHz reference input of the synthesizer. The 1.5GHz clock required for the TX/RX trigger generation is derived from a divider output in the PLL loop. An on-chip JTAG TAP interface is used to input the control bits of the pulse generator.

In the RX, a two-stage cascode LNA with inductive degeneration is used for each band, and the outputs of the second stages are combined into a dual-band LC filter (Fig. 18.2.2), thereby allowing sharing of the downconversion chain by the two bands. Although only one path is active at a time, an interferer from the other input can desensitize the broadband mixer. Therefore, high isolation is necessary from each input to the LNA output in the off state. To this end, a dedicated first stage is used in each path. Furthermore, series T-lines $T_{1,2}$ improve isolation between the two paths by resonating out the parasitic capacitances at collector terminals of the second-stage cascode transistors which, in turn, results in an increase in the amplifier gain. The measured off-state isolation between each LNA input and the LNA output is better than 30dB. The LNA is followed by broadband double-balanced I/Q mixers with resistive degeneration, VGAs and integrators. Pulse formers generate the reference pulses for correlation with the received pulses in the mixers. The 22-to-29GHz/77-to-81GHz RX achieves 35/31dB gain, 4/5dB DSB NF and better than 30dB isolation between the two bands. It draws 43/65mA from 2.5V.

In the TX, a dual-band pulse former, which is shared between the 24/79GHz paths, drives the PAs (Fig. 18.2.3). The pulse former circuit, comprising of a Gilbert-type mixer with a dual-band LC tank, upconverts the baseband pulse to the 24/79GHz transmit carrier frequency. Dual-band resonant loads increase the gain and provide bandpass filtering at 24GHz and 79GHz to restrict the signal within the regulated transmit mask. LO leakage is reduced by terminating one of the differential pair outputs in an AC short circuit and by applying the LO inputs to the lower differential pair [4]. The two PAs consist of common-emitter stages operating in Class-A mode. The 24GHz PA achieves 18dB gain and 14.5dBm P_{1dB} . The 79GHz PA has a gain of 10dB and a P_{1dB} of 10.5dBm. The 24/79GHz PAs achieve 3dB BWs of 21-to-28GHz/75-to-80.5GHz. A cascode pre-driver precedes the three-stage 79GHz PA to improve isolation between the two paths. Input/output and inter-stage matching networks are designed using T-lines and MIM capacitors.

The dual-band frequency synthesizer is an improved version of the chip presented in [6]. Outputs of the 24GHz and 79GHz VCOs are multiplexed into the input of an injection-locked divide-by-3 circuit, which acts as a divider for the 79GHz input and as a tuned buffer for the 24GHz input. The quadrature LO required for Doppler detection in the RX is generated by using coupled T-lines with an electrical length of $\lambda/4@24$ GHz and close to $3\lambda/4@79$ GHz. The T-lines are loaded with varactors to fine tune the resonant frequency. The synthesizer achieves a locking range of 23.8 to 26.95GHz/78.4 to 81.1GHz and a phase noise of $-114/-100.4$ dBc/Hz@1MHz offset.

The TRX chip performance is measured using a coaxial setup for 24GHz and a waveguide-based setup for 79GHz. In addition to circuit breakouts, *in-situ* probing is also enabled using pads that are absorbed as part of the design. The measured transmitter output pulse transients and spectra for both bands are shown in Fig. 18.2.4; the pulse width is chosen for full-bandwidth (7GHz for 24GHz band, and 4GHz for 79GHz band) operation and the PLL output frequency is set at the center of the band (25.5/79GHz). The 24GHz output is measured directly on a sampling oscilloscope, while the 77GHz output is first downconverted to a 4GHz IF using a WR10 waveguide mixer (the spectrum of the 79GHz pulse shown in Fig. 18.2.4 was scaled back to W-band for clarity). Spectral nulls corresponding to pulse widths of about 300ps for the 24GHz pulse and 1ns for the 79GHz pulse are readily seen in Fig. 18.2.4.

The complete measured performance of the TRX is summarized in Fig. 18.2.5. Radar functionality of the TRX is verified using the loopback measurement setup depicted in Fig. 18.2.6. In the 24GHz band, the TX output is attenuated and directly fed back to the RX input. Due to mechanical constraints of the waveguides, for the 79GHz band, the TX output is first downconverted to a 4GHz IF, upconverted back to 79GHz, attenuated and then applied to the RX input. The RX correlation function, plotted in Fig. 18.2.6, is determined by varying the delay between TX and RX triggers in the pulse generator. Due to transmit mask constraints at 24GHz and high path loss at 79GHz, multiple pulses need to be integrated to raise the signal above the noise floor. This is demonstrated in measurement results of Fig. 18.2.6, which shows the integrator output after coherent integration of 500 pulses for each delay setting. A 1ns pulse is generated, corresponding to a 15cm range resolution, and the delay is varied in 200ps steps, corresponding to 3cm range accuracy. For this measurement, the power level at the attenuator output is set to -80 dBm.

The TRX achieves a low power dissipation of 0.51W in the 24GHz band and 0.615W in the 79GHz band, compared to 4.1W reported for the 79GHz TX in [4] for short-range applications. A die micrograph of the 3.9 \times 1.9mm² radar TRX chip is shown in Fig. 18.2.7.

Acknowledgement:

The authors thank Jazz Semiconductor for chip fabrication and Fujitsu Labs of America for the generous support. They acknowledge contributions by Babak Javid of WiLinX and helpful suggestions by the IBM mm-wave team, Abbas Komijani of Atheros Communications and Chun-Cheng Wang of UC Irvine. This work was supported in part by an NSF grant under contract CRI-0551735.

References:

- [1] I. Gresham, et al., "Ultra-WideBand Radar Sensors for Short-Range Vehicular Applications," *IEEE Trans. Microwave Theory and Techniques*, vol. 52, no. 9, pp. 2105-2122, Sept. 2004.
- [2] V. Jain, S. Sundararaman, and P. Heydari, "A CMOS 22-29GHz Receiver Front-End for UWB Automotive Pulse-Radars," *IEEE Custom Integrated Circuits Conf.*, pp. 757-760, Sept. 2007.
- [3] A. Natarajan, A. Komijani, X. Guan, et al., "A 77GHz Phased-Array Transceiver With On-Chip Antennas in Silicon: Transmitter and Local LO-Path Phase Shifting," *IEEE J. Solid-State Circuits*, vol. 41, no. 12, pp. 2807-2819, Dec. 2006.
- [4] S. Trotta, H. Knapp, D. Dibra, et al., "A 79GHz SiGe Bipolar Spread-Spectrum TX for Automotive Radar," *ISSCC Dig. Tech. Papers*, pp. 430-431, Feb. 2007.
- [5] European Radiocommunications Office, EC Decision 2005/50/EC, "Commission Decision of 17 January 2005 on the Harmonisation of the 24 GHz Range Radio Spectrum Band for the Time-Limited Use by Automotive Short-Range Radar Equipment in the Community," *Official Journal of the European Union*, Jan., 2005. Accessed on Nov. 16, 2008, <<http://www.ero.docdb.dk/Docs/doc98/official/pdf/200550EC.PDF>>
- [6] V. Jain, B. Javid, and P. Heydari, "A 24/77GHz Dual-Band BiCMOS Frequency Synthesizer," *IEEE Custom Integrated Circuits Conf.*, pp. 487-490, Sept. 2008.

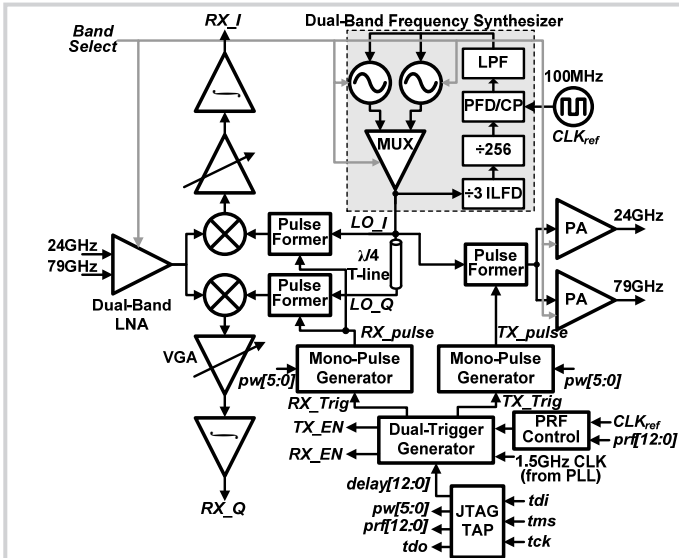


Figure 18.2.1: Block diagram of the 24/79GHz dual-band transceiver.

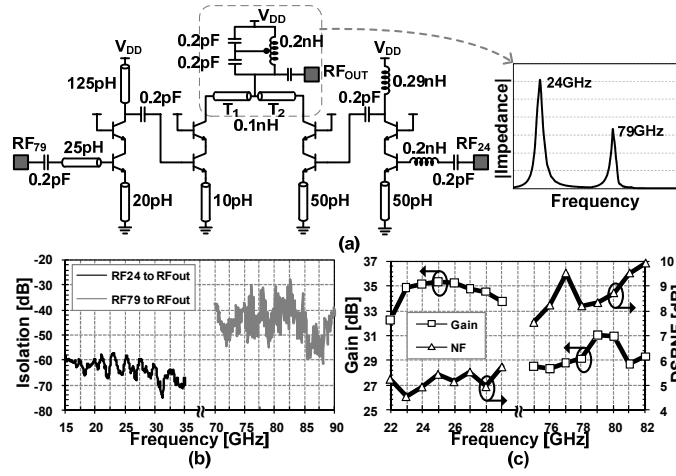


Figure 18.2.2: (a) Dual-band LNA schematic, (b) measured off-state isolation between LNA inputs and output, and (c) measured RX conversion gain and noise figure.

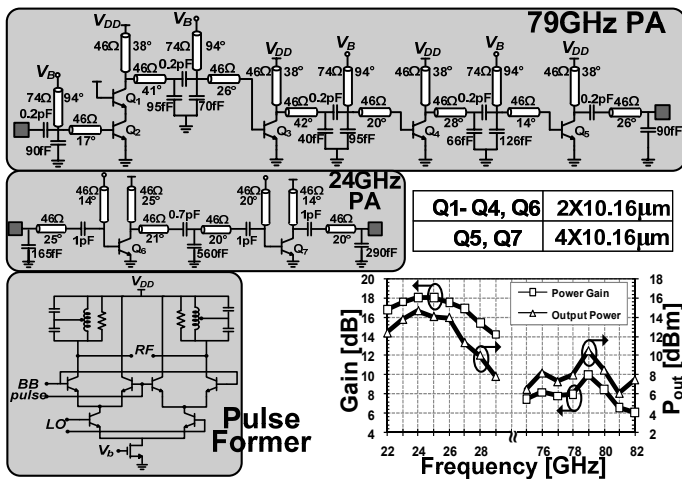


Figure 18.2.3: Pulse former and PA schematics with measured PA gain and output power.

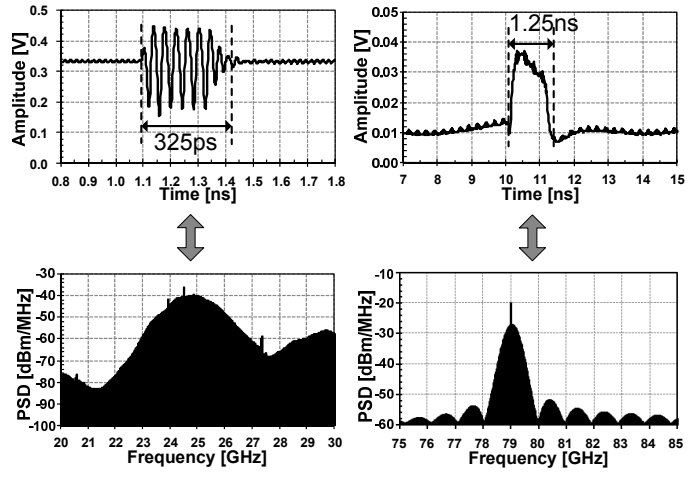


Figure 18.2.4: Measured transmitter output pulses and their spectra.

Receiver (24/79GHz)		Transmitter (24/79GHz)	
Conversion Gain	35/31dB	PA Gain	18/10dB
DSB Noise Figure	4.5/8dB	Output P1dB	14.5/10.5dBm
Input Return Loss	< -10dB	Frequency Synthesizer (24/79GHz)	
Output Return Loss	< -15dB	Phase Noise @ 1MHz	-114/-100.4dBc/Hz
LO-to-RF leakage	< -70dB	Locking Range	23.8-26.95/78.4-81.1GHz
LO-to-IF leakage	< -38dB	Spurs	< -47dBc
Input P _{1dB}	-33.2/-30.7dBm	Power Dissipation (24/79GHz)	
I/Q Mismatch	< 2°/5° < 1.1/1.5dB	RX	107.5/162.5mW
Technology	0.18μm BiCMOS	TX	312.5/332.5mW
Die Size	3.9mm×1.9mm	Frequency Synthesizer	90/120mW
Supply Voltage	2.5V (Analog) 1.8V (Digital)	Total	510/615mW

Figure 18.2.5: Dual-band radar transceiver performance summary.

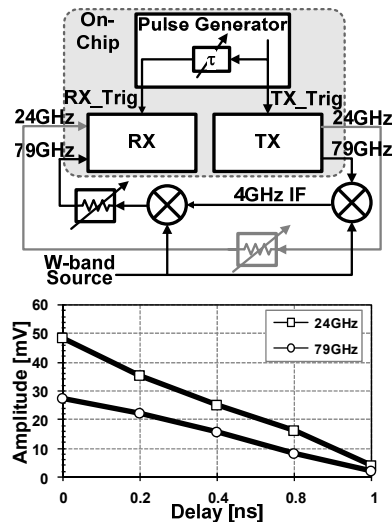
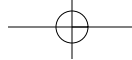


Figure 18.2.6: Transceiver loopback measurement setup and measured correlation function for a 1ns pulse.



ISSCC 2009 PAPER CONTINUATIONS

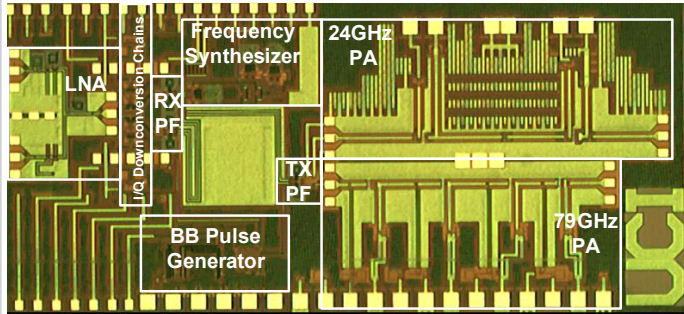


Figure 18.2.7: Die micrograph of the dual-band transceiver.

